OFFICE OF NAVAL RESEARCH

GRANT N00014-89-J-1178

R&T Code 413Q001-05

TECHNICAL REPORT NO. #38

An Kinetics Study of The Electron Cyclotron Resonance Plasma Oxidation of Silicon

by

J. Joseph , Y. Z. Hu and E. A. Irene
Department of Chemistry, CB# 3290
University of North Carolina
Chapel Hill, NC 27599-3290

Submitted to the
Journal of the Electrochemical Society

SECURITY CLASSIFICATION OF THIS PAGE

REPORT DOCUMENTATION PAGE

1a. REPORT SECURITY CLASSIFICATION unclassified	1b. RESTRICTIVE MARKINGS
2a. SECURITY CLASSIFICATION AUTHORITY	3. DISTRIBUTION/AVAILABILITY OF REPORT Approved for public release; distribution unlimited.
2b. DECLASSIFICATION/DOWNGRADING SCHEDULE	
4. PERFORMING ORGANIZATION REPORT NUMBER(S) Technical Report # 38	5. MONITORING ORGANIZATION REPORT NUMBER(S)
6a. NAME OF PERFORMING ORGANIZATION UNC Chemistry Department 6b. OFFICE SYMBOL (If applicable)	7a. NAME OF MONITORING ORGANIZATION Office of Naval Research (Code 413)
6c. ADDRESS (City, State and ZIP Code) CB# 3290, Venable Hall University of North Carolina Chapel Hill, NC 27599-3290	7b. ADDRESS (City, State and ZIP Code) Chemistry Program 800 N. Quincy Street Arlington, Virginia 22217
8a. NAME OF FUNDING/SPONSORING ORGANIZATION Office of Naval Research 8b. OFFICE SYMBOL (If applicable)	9. PROCUREMENT INSTRUMENT IDENTIFICATION NUMBER Grant #N00014-89-J-1178
8c. ADDRESS (City, State and ZIP Code) Chemistry Program 800 N. Quincy Street, Arlington, VA 22217	10. SOURCE OF FUNDING NOS. PROGRAM ELEMENT NO. / PROJECT NO. / TASK NO. / WORK UNIT NO
11. TITLE (Include Security Classification) A KINETICS STUDY OF THE ELECTRON CYCLOTRON RESONANCE PLASMA OXIDATION OF SILICON	
12. PERSONAL AUTHOR(S) J. Joseph*, Y. Z. Hu and E. A. Irene	
13a. TYPE OF REPORT Interim Technical 13b. TIME COVERED FROM _____ TO _____	14. DATE OF REPORT (Yr., Mo., Day) November 1991 15. PAGE COUNT 36
16. SUPPLEMENTARY NOTATION Journal of the Electrochemical Society	
17. COSATI CODES FIELD / GROUP / SUB. GR.	18. SUBJECT TERMS (Continue on reverse if necessary and identify by block number)

19. ABSTRACT (Continue on reverse if necessary and identify by block number)

The electron cyclotron resonance plasma oxidation of Silicon was investigated using in-situ during process static spectroscopic ellipsometry and dynamic real time ellipsometry at oxidation temperatures between 80°C and 400°C and at various applied bias'. Successful optical modeling of the ellipsometric data was accomplished using a two layer model, in which the top layer is a pure silicon dioxide film over an interface layer. The kinetics results are compatible with the Cabrera-Mott theory for the oxidation by charged species in the limit of low electric field. The effect of applied bias suggests that the oxidizing species is O^-. The energy activation is 0.18 eV, substantially lower than the thermal oxidation value.

20. DISTRIBUTION/AVAILABILITY OF ABSTRACT UNCLASSIFIED/UNLIMITED ☒ SAME AS RPT. ☐ DTIC USERS ☐	21. ABSTRACT SECURITY CLASSIFICATION Unclassified
22a. NAME OF RESPONSIBLE INDIVIDUAL Dr. Mark Ross	22b. TELEPHONE NUMBER (Include Area Code) (202) 696-4410 22c. OFFICE SYMBOL

DD FORM 1473, 83 APR EDITION OF 1 JAN 73 IS OBSOLETE.

SECURITY CLASSIFICATION OF THIS PAGE

Send ECS Sept 12, 1991 EM

A Kinetics Study of the Electron Cyclotron Resonance Plasma Oxidation of Silicon

J. Joseph[a], Y.Z. Hu and E.A. Irene
Dept. of Chemistry, CB# 3290
University of North Carolina
Chapel Hill, NC 27599-3290

Abstract

The electron cyclotron resonance plasma oxidation of Silicon was investigated using in-situ during process static spectroscopic ellipsometry and dynamic real time ellipsometry at oxidation temperatures between 80°C and 400°C and at various applied bias'. Successful optical modeling of the ellipsometric data was accomplished using a two layer model, in which the top layer is a pure silicon dioxide film over an interface layer. The kinetics results are compatible with the Cabrera-Mott theory for the oxidation by charged species in the limit of low electric field. The effect of applied bias suggests that the oxidizing species is O^-. The energy activation is 0.18 eV, substantially lower than the thermal oxidation value.

a. Permanent Adress: Ecole Centrale de Lyon, Ecully, France.

Introduction

Present silicon technology requires low temperature processing. For this purpose the electron cyclotron resonance, ECR, plasma appears to be a promising processing tool, because the high ionization ratio associated with ECR, yet the low energy ionic species enables low processing temperatures with low damage[1]. At the present time most ECR studies are with film deposition[2,3] and etching[4,5], and relatively fewer studies of Si oxidation are available[6,7,8,9,10]. In our previous study[11] we investigated the damage associated with ECR oxidation of Si, and found that the damage is due to the oxidation reaction itself and not typical of ion bombardment damage, and we reported bias effects on the oxidation kinetics. Since this technique enables the production of thin oxides at low temperatures, the present study is aimed at understanding the mechanism for oxidation, and includes ECR plasma oxidation of Si at temperatures between about 80°C and 400°C using in-situ ellipsometry for the characterization. In order to obtain a reliable description of the growth of the oxide layer, we performed two complementary in-situ ellipsometric measurements: static spectroscopic and dynamic real time measurements at a fixed wavelength. The former technique enables a precise determination of the correct optical model and the determination of model parameters such as damage layer thickness, and film and damage layer composition, and the latter technique provides dynamic information on film growth as a function of oxidation time. We

found that the sample bias and temperature are the main parameters for understanding the oxidation kinetics. Our previous study[11] revealed that the ECR oxidation produced a complex layer, and that multilayer modeling is required.

Experimental Procedures

Figure 1 shows a diagram of the apparatus which consists of a high precision rotating analyzer spectroscopic ellipsometer system with an independent vacuum process chamber equipped with a homemade ECR plasma source; this apparatus was previously discussed[12,13]. The plasma conditions used were: 300 W input power at a frequency of 2.45 GHz , oxygen pressure of 5×10^{-4} torr . The distance from the microwave cavity to the silicon sample wafer was 20 cm.

The spectroscopic ellipsometer measurements were taken at 41 photon energies between 2.5 and 4.5 eV. This spectral region was chosen because it contains the main features of the optical spectrum of silicon, namely, the two interband transition at 3.4 and 4.2 eV. At lower energy the value of Δ for bare Si with a thin oxide is close to 180° and therefore difficult to measure with a rotating analyzer ellipsometer[14] and, at higher energy the sensitivity of the system decreases due to insufficient light intensity. For all the spectra the polarizer was set at 25° which optimized the accuracy throughout the spectrum. For each sample the offsets of analyzer and polarizer were redetermined. This was necessary to maintain the highest accuracy, because a small misalignment of the sample stage occurred with sample changes. Each spectroscopic measurement takes about 10 min and during the

measurement the plasma was stopped. For the oxides grown above room temperature the spectra were obtained at room temperature after cooling the sample. This was done because of the unavailability of reliable optical data for all the components present for the higher temperatures. At each wavelength a Fourier analysis of the periodic output signal yielded the ellipsometric parameters Δ and Ψ from which the complex reflection coefficient ρ_{exp} is obtained:

$$\rho = \tan\Psi \exp(i\Delta)$$

From a literature database for the known constituents of the film and substrate ρ_{cal} is calculated and compared with ρ_{exp} and as a figure of merit for comparison, an unbiased estimator, δ, is calculated from the relationship[15]:

$$\delta = \left[\frac{1}{N-P-1}\Sigma|\rho_{exp}-\rho_{cal}|^2\right]^{\frac{1}{2}}$$

where N is the number of wavelengths sampled, and P the number of unknown parameters. A minimizing procedure gives the best fit parameters which are film thicknesses and percents for the constituents at the 90 % confidence interval. Throughout this work the unbiased estimators are in the range 0.003-0.008. A value outside this range was considered as an indication of problems in the measurement or a discrepancy in the modelling. The real time single wavelength measurements were carried out at 340 nm (3.65eV). This energy was chosen for several reasons. First, the values of

Δ and Ψ for the bare silicon and thin oxides are in a region where the accuracy of the rotating analyzer ellipsometer is good. Second, the dependance of the dielectric function of silicon on sample temperature is the smallest. Figure 2 shows our spectroscopic ellipsometric measurements for a bare silicon wafer after chemical cleaning at three temperatures, and these data agree with previous results [16]. It is seen that the spectra are coincident at about 3.65 eV. This discovery enables the attainment of highly accurate ellipsometric data despite temperature changes that occur during processing. For sample temperatures above ambient the heating is regulated; but for measurement without applied heating (refered to here as room temperature) the temperature floats to about 80° C depending on the duration of the oxidation experiments. With the use of the 3.65 eV photon energy we are able to ignore the temperature changes in the optical properties of Si and obtain the changing thickness of the oxide layer. Third, there is high sensitivity to the thickness variation of the oxide layer. Figure 3 shows a typical variation of the pseudo dielectric function for different oxidation times, and at 3.65 eV a proportional change is seen with increasing thickness. Lastly, at this energy the transparency of the oxide is high and Si is low rendering the two major components optically dissimilar hence improving the measurement contrast.

Oxidations were performed using about 10 ohm cm p-Si (100) oriented single crystal Si wafers that were cleaned using the RCA procedure[17], and immediately placed in the load lock of the vacuum

chamber. For all samples an initial spectrum was obtained prior to ECR processing, in order to insure the same starting surface. The initial spectra have shown that the cleaning procedure is reproducible and that the cleaned samples could be precisely described by a one film model using the Bruggeman effective medium approximation[18], BEMA, to be discussed below, and with the film composed of equal percentages of SiO_2 and amorphous silicon and with a thickness close to 1 nm on a crystalline Si substrate. We believe that the necessity to model the native film as a mixture of oxide and a-Si is an indication of some roughness and/or contamination.

Optical Modelling

For the analysis of the ellipsometric measurements different optical models were used for the spectroscopic data and the single wavelength data. This was done for ease of extracting the desired parameters.

Spectroscopic ellipsometry has been shown to yield reliable information for complex films with the use of stratified layer models[19]. Each of the layers is either a medium for which the optical properties are known, such as SiO_2, or where the properties can be described by a mixture of components. For this latter case, the optical properties are determined from the dielectric functions of the components and the volume fraction using the Bruggeman effective medium approximation, BEMA. The BEMA assumes a discrete but compositionally inhomogeneous film where the state of aggregation of the components is smaller that the wavelength of light but not atomic points.

In order to limit the number of parameters, we assumed that the entire oxide overlayer can be described by no more than two discrete layers and that each layer was composed of no more than two components. Therefore, the unknown parameters in the model was limited to four: two thicknesses and two volume fractions. The layers were assumed to be composed of one or two of following components with well known dielectric functions: c-Si[20], a-Si[21], SiO_2[22] and voids.

Four sensible models shown in Figure 4 were evaluated and the

results are summarized in Table I. From column 2 which shows the quality of the fit, in terms of the unbiased estimator, δ, it appears that model 4, made up of a pure SiO_2 topmost layer and an interface layer composed of SiO_2 and a-Si, always yields the best fit in terms of the lowest unbiased estimator, δ. This table also shows the errors associated with the parameters. These values are typical of the results obtained throughout this work. Sometimes voids added to the topmost SiO_2 layer made a small improvement, however always with a volume fraction not larger than the associated error. For simplicity this fact was ignored and pure SiO_2 was used for the topmost layer. In all of our results the volume fractions of SiO_2 and a-Si in the interface layer were close to 50 %. Thus the relevant parameters of this model are the thickness of the top SiO_2 film, L_{ox}, and the thickness of the interface layer, L_{int}. For some few oxidation parameters significant deviations to this model were observed and these will be mentioned later.

In order to interpret the single wavelength measurements in terms of oxidation kinetics (SiO_2 thickness versus oxidation time) a trajectory method was used[23]. In this procedure a measured (pseudo) refractive index for the starting cleaned Si surface was used and the complex multilayer system is simulated by one layer with an adjusted composite refractive index. For this calculation the index of the substrate is calculated from the first experimental point, and using this value a trajectory in the Δ,Ψ plane corresponding to the growth of the layer with an arbitrary

index is compared to the experimental points. For this comparison an error function is defined as the sum of the distance between the experimental points and the calculated trajectory in the Δ,Ψ plane. With the use of a minimization procedure the index of the layer is varied to obtain the minimum of the error function. The thickness of the layer corresponding to each experimental point is assumed to be that of the closest point to the trajectory. From this procedure a calculated value for the index of the layer is also obtained. This value could give some information about changes in the layer during oxidation, but it is not as precise as the spectroscopic results. We have verified that there is no measurable difference for the growth of a thin oxide between this one layer model using an effective index for the substrate, and the more exact two layer model, where the substrate is described by a native oxide layer over bare c-Si. It is worth noting that the thickness of the layer in the one layer model is only the thickness above the initial layer, but in the two layer model the thicknesses of the layers are measured from the bare ideal silicon.

Experimental Results

Oxidation at Room Temperature for Different Sample Bias'.

We found that an applied (relative to ground) sample potential of -30V halted film growth and the plasma became unstable above +60V, hence these values provide the limits for this investigation. The floating potential of the ECR plasma with no applied bias puts the sample at about -20V with respect to the plasma potentiel. By

keeping oxidation experiments under 30 min the maximum sample temperature was less than 80°C for the room temperature mesurements. Figure 5 shows, the evolution of the ellipsometric measurements at different bias' in the Δ,Ψ plane during the first 20 minutes of the room temperature oxidation. The results for 60V bias have not been plotted, because the trajectory is too close to the 30 V trajectory. For ease of comparison, the experimental trajectories have been shifted a small amount (the shift is within the experimental uncertainty of the measurement) to coincide at the same starting point. In this Figure the solid lines correspond to a calculation performed with a one layer model using the result of the trajectory method for the optical index of the layer. The evolution of the oxide film thicknesses as a function of the time for different bias values are shown in Figure 6. From these results and also from spectroscopic measurements that follow, performed during the very beginning of the oxidation, it appears that two different oxidation regimes occur during plasma oxidation.

The first regime corresponds to about the first five degrees shift of Δ downwards, or about 2nm in oxide thickness. The key feature of this early oxidation regime is that the extent of the oxidation is virtually bias independent. The bias does, however, affect the duration of this regime: 20s duration with negative bias to 90s with a positive bias. The time dependence suggests that ion bombardment is the main effect during this period. With the high concentration of positive ions in the ECR plasma, the negative

sample bias would enhance the positive ion energy, and therefore the importance of ion bombardment. The effect of the bombardment can also be deduced from the difference between the experimental points and the theoretical calculation in Figure 5 where it is seen that this difference is greater for the 0 and the -30 V bias. Spectroscopic measurements for the positive bias process at intermediate times revealed that the best model for the initial regime is a one layer model with an equal fraction of a-Si and SiO_2, i.e. the same as for the initial layer after cleaning.

The second oxidation regime corresponds mainly to the growth of the SiO_2 film as obtained from the spectroscopic measurements. During this regime the experimental points are very close to the theoretical trajectory for all bias'. The different solid line trajectories in Figure 5 correspond to the use of different calculated SiO_2 indices. The real part of the refractive index, n, is close to the value usually given for thermal SiO_2, but there is a small non zero imaginary part, k. This imaginary part increases as the bias decreases, and thus provides a clockwise rotation of the experimental data in Figure 5. This result could be explained either by a concomitant increase of the thickness of the interface layer and/or by some inclusion of unoxidized species in the oxide layer during the growth. The spectroscopic ellipsometry measurements are concordant and show that there is an increase of the concentration of unoxidized optically absorbing species during growth in the layer that decreases with positive bias. The volume fraction of a-Si in the interface layer is close to 50% for

positive or the zero bias, but for the negative bias experiments it was close to 75% in concordance with the higher k value obtained with the trajectory method.

The evolution of the thicknesses as a function of the oxidation time, obtained using the trajectory method, during the first 20 min is shown in Figure 6. The spectroscopic measurements were used to obtain the evolution of the thicknesses during the second regime. For all these spectra Model 4 always yielded the best fit . The results of this analysis are plotted in Fig 7. As previously mentionned the volume fraction of amorphous silicon in the interface layer was found close to 50% for all these spectra. The thicknesses of the interface layer are also constant and nearly independant of bias. The deviations are withhin the 90% confidence limits which is about 0.5 nm.

Oxidation at Different Temperatures

With a bias of +30V, corresponding to the middle of the useful bias range, ECR oxidations were performed at 200°C, 300°C and 400°C. The results from the single wavelength kinetic measurements are shown in Figure 8. From these results it is clear that the shape of the growth rate is similar for all the temperatures; and the results of the spectroscopic measurements are also similar to the room temperature results. However, there is a difference in the results of the modeling of the spectroscopic measurements. For the longest oxidation times yielding oxides thicker than 25nm at 300°C and 400°C, voids had to be added to the oxide layer to obtain acceptable unbiased estimator values. This result points out that

even our best model has limitations.

Discussion of Results.

For thermal oxidation of Si there exist significant evidence that the linear parabolic oxidation model adequately describes the appropriate physics of oxidation and yields a reasonable approximation to the kinetics[24]. In this model there are two oxidation regimes: first in the early regime the oxide growth is limited by the reaction at the Si surface, and later by the diffusion of the oxidizing species through the oxide. In the ECR plasma oxidation at room temperature the moving species are most likely different from those of thermal oxidation and the transport of these species is not only due to Fickian diffusion, but more importantly to the drift of charged species in the electric field. Many of these kind of models also yield a linear parabolic rate law[25] and, as a consistency check, Figure 9 shows a representative plot of the oxide thickness vs the square root of the time for one of our thicker oxide data sets. It is seen that after the first few data points, the results fit this time dependence. Thus, all our results are interpreted with a simple relationship:

$$L^2=Bt+C$$

Where L and t are oxide thickness and oxidation time, respectively and B and C constants. Since all the curve fitting procedures using this equation give an insignificant value for C, only B was used for the comparison with the models. Therefore, using the

total film thickness, $L_t = L_{ox} + L_{int}$ as the thickness of the layer, Figures 10 and 11 show the kinetics data (the points are only for the static spectroscopic data) and the linear fits which provide the parabolic coefficient B. In Figure 11 the -30V bias curve does not follow the square root relationship well. Both the single wavelength and the spectroscopic measurements show that after a fast initial regime, the thickness remains nearly constant. It was also shown above that for this bias the layer is far from a transparent oxide layer, hence the mechanism is not simply oxide growth and the kinetic results are not useful for comparison with the other results.

According the Cabrera-Mott theory for oxidation by charged species in the limit of the low field, the growth rate law[26] is given by:

$$L^2 = C_1 \mu V_{ox} t + C_2$$

where L is the thickness , t the oxidation time , C_1 and C_2 are constants, V_{ox} is the potential drop across the oxide film, μ is the mobility which is related to the diffusion coefficient D by the Einstein relationship:

$$ZeD = \mu kT$$

Where Ze is the electric charge of the ion, T the temperature and k the Boltzmann constant. The diffusion coefficient also depends on the temperature T and the activation energy E_a by a classical Arrhenius relationship:

$$D=D_0\exp\left[-\frac{E_a}{kT}\right]$$

Using all these relationships the growth law is:

$$L^2=C_1'D_0\exp\left[-\frac{E_a}{kT}\right]\frac{V_{ox}}{kT}t+C_2$$

where C_1' is a new constant. In order to compare our experimental results to this model, the dependance of the growth rate with the temperature and the bias is examined. This theory predicts that the product of the temperature and the parabolic coefficient follows an Arrhenius expression, and this is confirmed for our results in Figure 12. The linear fit of these data yields an activation energy of 0.18 eV. This result which is close to previous results of 0.25 eV[8], is notably lower that the activation energy for thermal oxidation (between 1.4 and 2.3 eV[24]) and clearly indicates a very different oxidation mechanism. Figure 13 shows that the parabolic coefficient is approximatively linearly dependant on the bias. However, it should be noted that V_{ox} is smaller than the applied sample bias V, because a significant part of the potential is dropped across the plasma sheath. This likely explains why even with a relatively high applied bias, the experimental results are close to the low field approximation. This explanation also implies that the relationship between V and Vox is linear at least in some range. The increase of the growth rate with the bias reveals that the oxidizing species are negative, but contrary to

electron density, the density of negative ionic species is low in the plasma. In order to explain our results, we consider a multi step kinetic process. The plasma electrons first react by a favored reaction with the O_2 to produce the molecular ion, O_2^-, that is less stable than O_2, hence provides the atomic species O and O^-. O^- can readily migrate through the oxide under a positive sample bias.

From the evolution of the interface layer during the oxidation the best optical description is as a mixture of oxide and of amorphous silicon. However, this description is not necessarily unique and one must consider that several known interface phenomena such as interface roughness, presence of suboxides, strained oxide or a combination, are all likely. From our measurements we cannot decide which of these are dominant, but from the optical model we know for sure that this interface layer is very different from a pure oxide and that its composition is almost constant. The largest part of this layer is formed during the early stage of the ECR oxidation and afterwards changes little. This layer behaves as a marker in that it neither moves toward the surface nor spreads out in the oxide layer during the oxidation. This strongly suggests that the ECR oxidation occurs between this layer and the outer surface where the oxidation results from the movement of both the Si outward as a cation in the interlayer and the oxidant species inward as O^-. In this hypothesis the interface layer is the result of the steady state flux of Si^+ through the first layer of the oxide. That this layer is not permeable to the

oxidant species is not readily explained. This model is compatible with the Cabrera-Mott theory which holds for anion or cation oxidation.

Conclusions

1. We have shown that the bias of the sample is an important parameter for ECR plasma oxidation. Positive bias increases the growth rate and decreases the interface layer thickness. The damage resulting from the plasma occurs during the early stage of the oxidation and can be reduced with positive bias.

2. The oxide layer obtained using ECR plasma exhibits a complex structure. From the spectroscopic ellipsometry measurements this film is composed of two layers: a pure silicon dioxide layer and an interface layer. Optically, the interface layer is composed of amorphous silicon and oxide but futher work is necessary to fully elucidate this layer.

3. The effect of the bias and the low activation energy (0.18 eV) for ECR oxidation definitively shows that the oxidizing species in plasma oxidation are different from those of thermal oxidation. The atomic ion O^- is the most probable oxidant species.

4. The growth rate can be modelled by a parabolic law. A parabolic relationship for the growth rate could be obtained with different models, but our results show the dependance of temperature and bias are close to the Mott-Cabrera theory for the oxidation by the charged species in the limit of the low electric field.

Acknowledgments

This work was supported by NSF through an Engineering Research Center at NC State University and by the Office of Naval Research,ONR. One of us (J.J) is grateful to NATO for a travel fellowship.

List of figures

Figure 1. Experimental set-up.

Figure 2. Pseudo-dielectric function of Si at different temperatures. The sample is a bare silicon wafer after chemical cleaning.

Figure 3. Typical Si pseudo-dielectric functions at different ECR oxygen plasma exposure times with bias of 30 V at room temperature.

Figure 4. Optical models considered.

Figure 5. Evolution of the ellipsometric Δ-Ψ trajectories during the first 20 minutes of oxidation for three bias and measured at a wavelength of 340 nm. The time between each experimental point is 20 seconds. The solid lines correspond to a model calculation.

Figure 6. Thicknesses of the grown oxide layer vs ECR oxidation time for four biases at room temperature. These curves are the result of data reduction at one wavelength using a one layer model.

Figure 7. Results from two layer modeling of in-situ spectroscopic ellipsometry data yielding the oxide thickness and the interface layer thickness. The measurements are for four biases at room temperature. The solid lines are only for ease of viewing. The interface thicknesses are represented by ■ , ▲ , ★ , ● , respectively, for 60, 30, 0 and -30 V applied bias'.

Figure 8. Thickness of the grown oxide layer vs ECR oxidation time for four temperatures. The bias is 30 V and a one layer model was used.

Figure 9. Thickness of the oxide layer, obtained from single wavelength ellipsometry measurements, as a function of the square root of ECR oxidation time, obtained at 300^{0}C for 30 V applied bias.

Figure 10. Square of oxide thickness vs the ECR oxidation time obtained from spectroscopic measurements for four temperatures measured with 30 V applied bias. Total thickness L_T is the sum of the oxide thickness and the interface thickness. The solid lines are the result of a linear fit.

Figure 11. Similar results as Figure 10, but for four applied bias measured at room temperature.

Figure 12. Arrhenius plot of product of the temperature and the parabolic coefficients deduced from linear fit of the curves in Figure 10. The solid line corresponds to a linear fit of the experimental data.

Figure 13. Parabolic coefficients vs applied bias .

Reference

1. J.E. Stevens, J.L. Cecchi, Y.C. Huang and R.L. Jarecki Jr, J. Vac. Sci. Technol. A9, 696 (1991).

2. J. Asmussen, J. Vac. Sci. Technol., A 7 , 883, (1989).

3. J.C. Barbour, H.J. Stein, O.A. Popov ,M. Yoder, and C.A. Outten. J. Vac. Sci. Technol. A 9 ,480 (1991).

4. M. Delfino, S. Salimian, and D.Hodul. J. Appl. Phys. 70 ,1712 (1991).

5. I.Suemune, A.Kishimoto ,K. Hamaoka ,Y. Honda, Y. Kan ,and M. Yamanishi, Appl. Phys. Lett. , 56, 2393 (1990).

6. J.R. Ligenza, J. Appl. Phys., 36, 2703 (1965).

7. T.Roppel, D.K. Reinhard, and J.Asmussen. J. Vac. Sci. Technol. B4 , 295 (1986).

8. C. Vinckier, P. Coeckelberghs, G. Stevens, M. Heyns, and De Jaegere. J. Appl. Phys.62, 1450(1987).

9. D.A. Carl, D.W. Hess, and M.A. Lieberman. J. Vac. Sci. Technol. A 8, 2924(1990).

10. S. Kimura, E. Murakani, K. Miyake, T. Warabisako, H. Sunami and T. Tokuyama. J. Electrochem. Soc.,132, 1460(1985).

11. Y.Z.Hu, J. Joseph and E.A. Irene, Appl. Phys. Lett., 59, 11 (1991).

12. J.W. Andrews, Y.Z. Hu and E.A. Irene, SPIE Proceedings of Multichamber and In-Situ Processing of Electronic Materials,1118,162(1990).

13. J.W. Andrews, Thesis, University of North Carolina, Chapel Hill, NC. 1990.

14. R.W. Collins, Rev. Sci. Instrum. 61,2069(1990).

15. D.E. Aspnes, J.B. Theeten and F. Hottier, Phys. Rev. B20,3992(1979).

16. P. Lautenschlager, M. Garriga, L. Vina, and M. Cardona. Phys. Rev. B 36, 4831(1987).

17. W. Kern and D.A. Puotinen , RCA Review, 31, 187(1970).

18. D.E. Aspnes, Thin Solid Film, 89, 249 (1982).

19. J.B.Theeten, R.P.Chang,D.E. Aspnes and T.E. Adams, J. Elelectrochem. Soc.,127, 378(1980).

20. D.E. Aspnes and A.A. Studna. Phys. Rev. B27. 985(1983).

21. D.E. Aspnes, A.A. Studna and E.Kinsbron. Phys. Rev. B 29, 768(1984).

22. I.H. Malitson, J. Opt. Soc. Am. 55, 1205(1965).

23. A. Gagnaire, J. Joseph and A. Etcheberry, J. Electrochem. Soc. 134,2476(1987).

24. E.A. Irene, CRC Crit. Rev. Rev. Sol. State Mat. Sci., 14,175(1988).

25. N. Cabrera and N.F. Mott, Rep.Prog. Phys. 12,163(1948).

26. F.P. Fehlmer, " Low-Temperature Oxidation ",Chap 2, John Wiley,New York,(1986).

Table I. Structural parameters and 90% confidence limits for the samples oxidized with ECR oxygen plasma at room temperature and bias voltages of +30 V (sample A) and +60 V (sample B). The models are shown schematically in Fig.4.

MODEL	$\delta x10^4$	L_{ox} (nm)	L_{int} (nm)	f_v(c-Si or a-Si) %
SAMPLE A				
1	167	10.6 ± 0.5	\	\
2	104	9.6 ± 0.4	\	4.6 ± 1.5
3	115	7.6 ± 1.5	2.0 ± 0.7	39 ± 60
4	48	7.8 ± 0.3	2.2 ± 0.2	54 ± 4
SAMPLE B				
1	138	7.3 ± 0.5	\	\
2	95	6.7 ± 0.4	\	4.2 ± 2
3	89	4.7 ± 5.6	2.1 ± 4	17 ± 21
4	47	5.1 ± 0.4	1.8 ± 0.4	56 ± 6

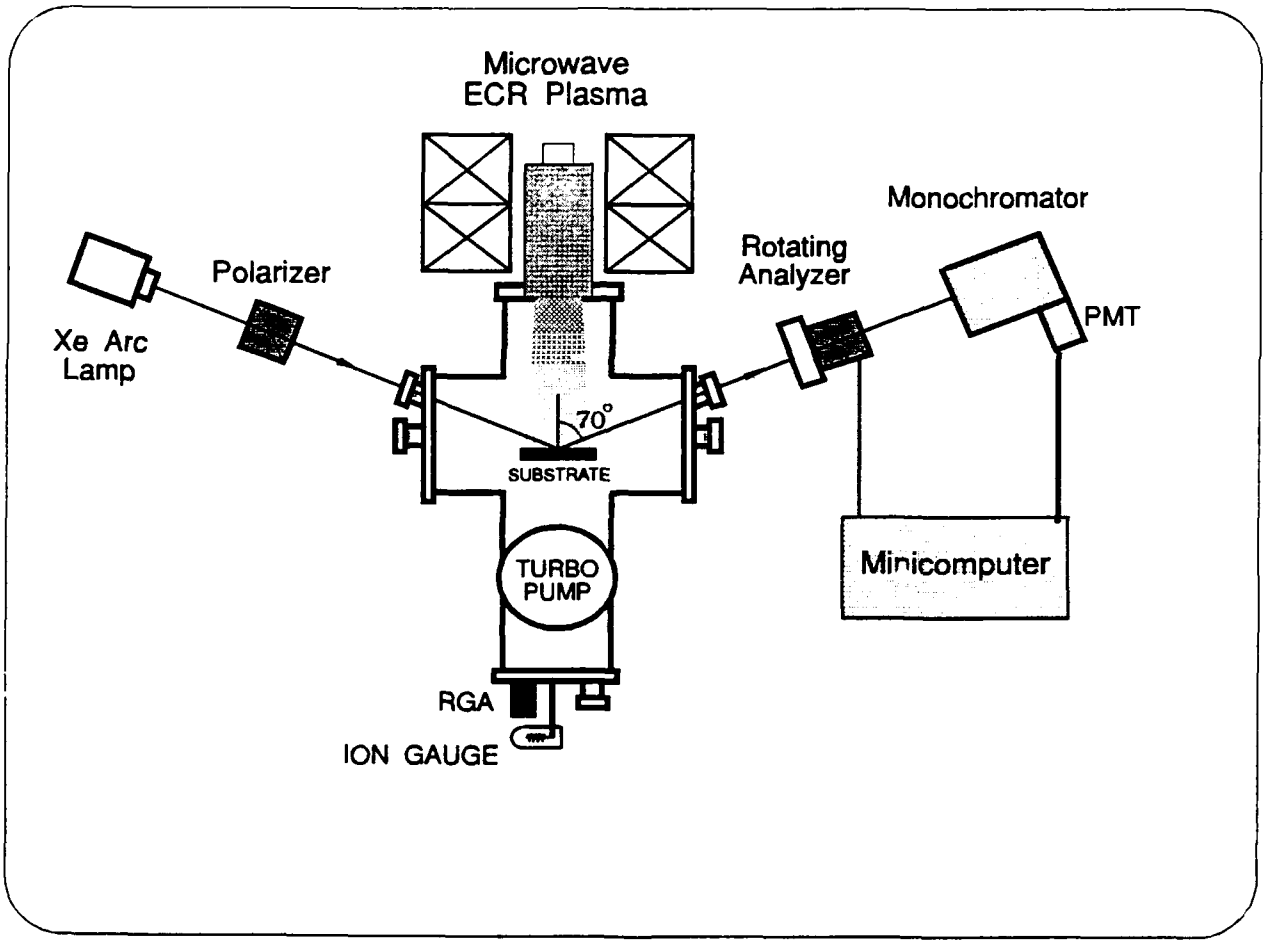
Microwave
ECR Plasma
Monochromator
Rotating
Analyzer
Polarizer
PMT
Xe Arc
Lamp
70°
SUBSTRATE
TURBO
PUMP
Minicomputer
RGA
ION GAUGE

Fig 1

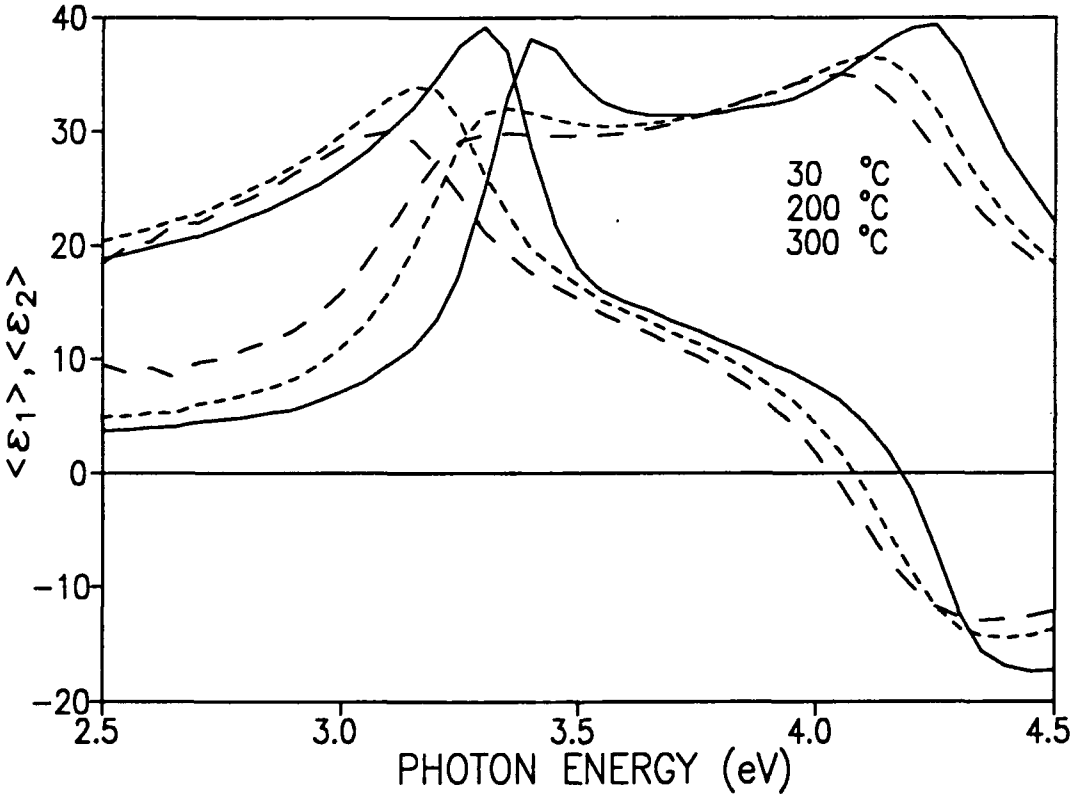
40
30
20
10
0
−10
−20
2.5
3.0
3.5
4.0
4.5
PHOTON ENERGY (eV)
<ε1>, <ε2>
30 °C
200 °C
300 °C

Fig 2

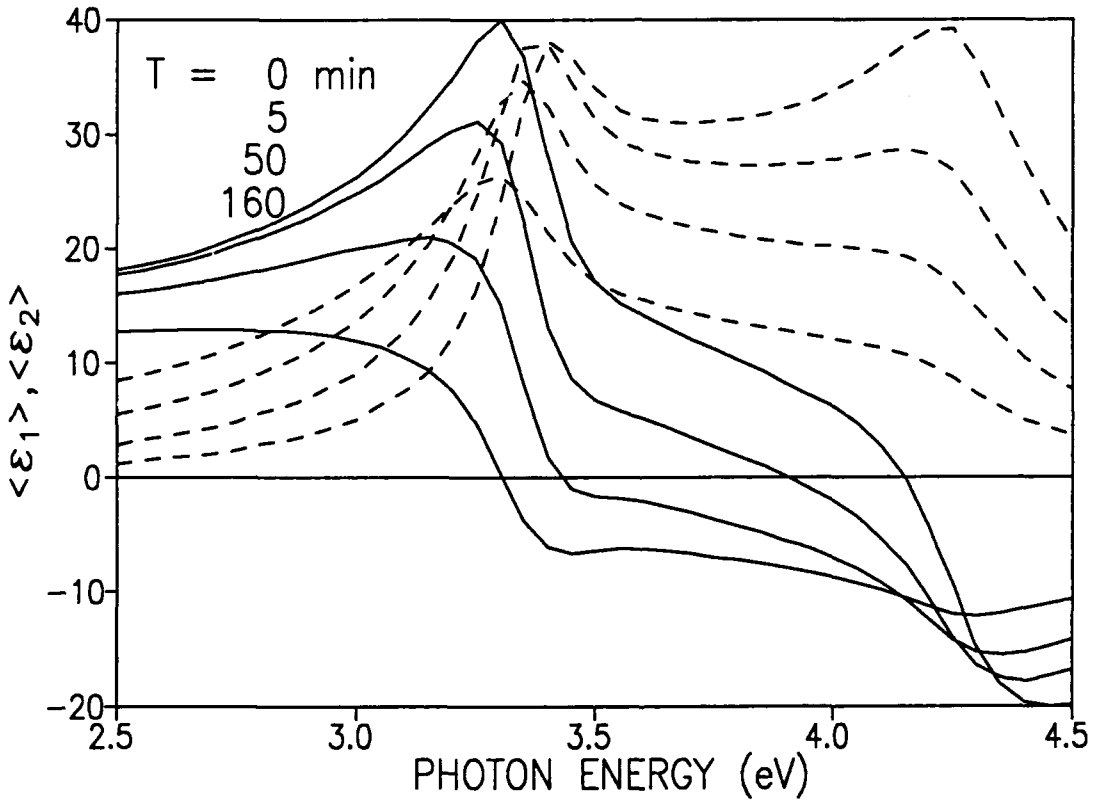
T = 0 min
5
50
160
40
30
20
10
0
−10
−20
2.5
3.0
3.5
4.0
4.5
PHOTON ENERGY (eV)
<ε1>, <ε2>

Fig 3

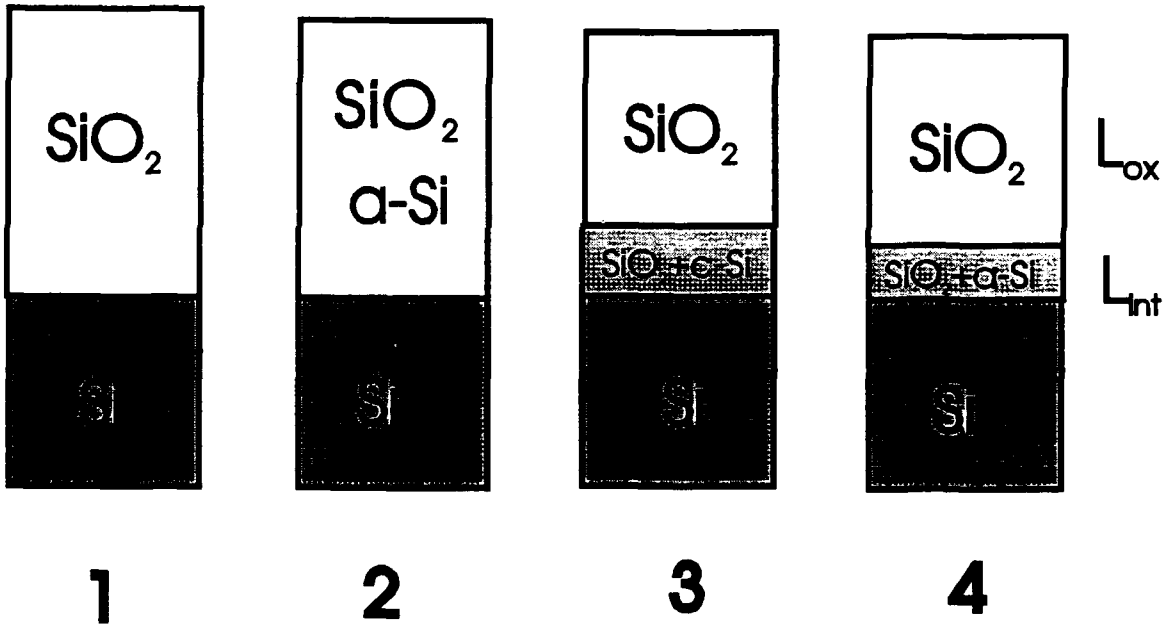
SiO2
Si
SiO2
a-Si
Si
SiO2
SiO2+c-Si
Si
SiO2
SiO2+a-Si
Si
Lox
Lint
1
2
3
4

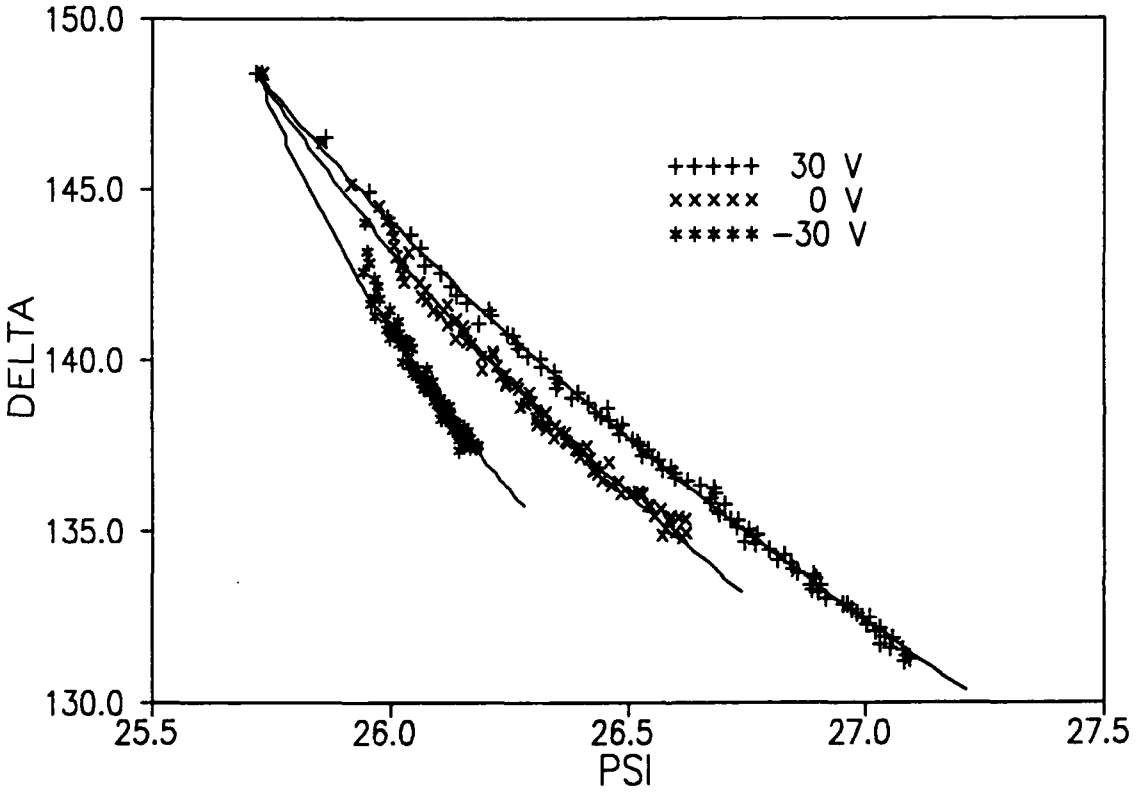
150.0
145.0
140.0
135.0
130.0
DELTA
25.5
26.0
26.5
27.0
27.5
PSI
+++++ 30 V
xxxxx 0 V
***** -30 V

Fig 5

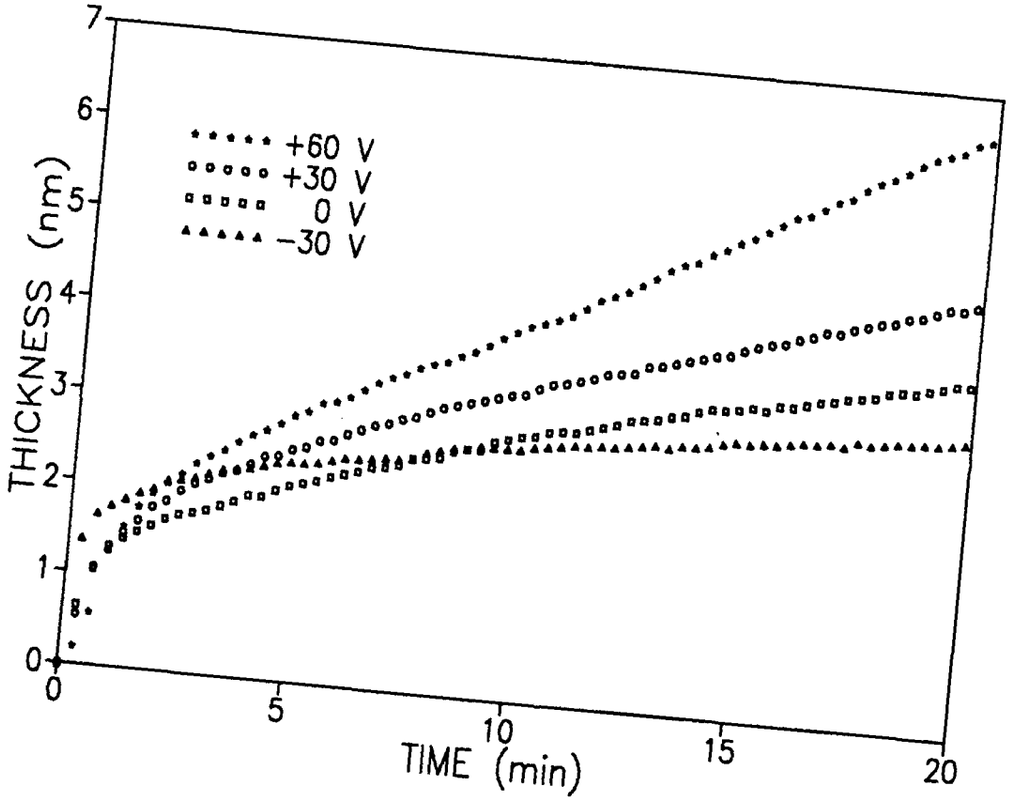

Fig 6.

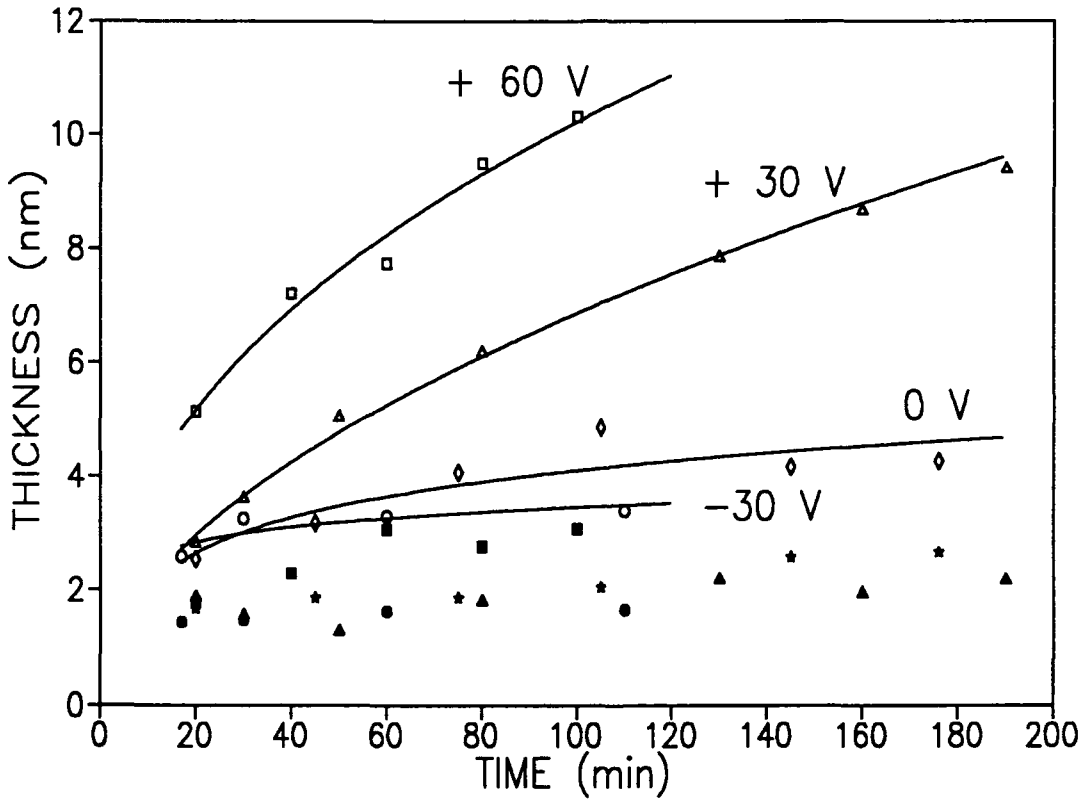
+ 60 V
+ 30 V
0 V
−30 V
THICKNESS (nm)
TIME (min)
0
2
4
6
8
10
12
0
20
40
60
80
100
120
140
160
180
200

Fig. 7

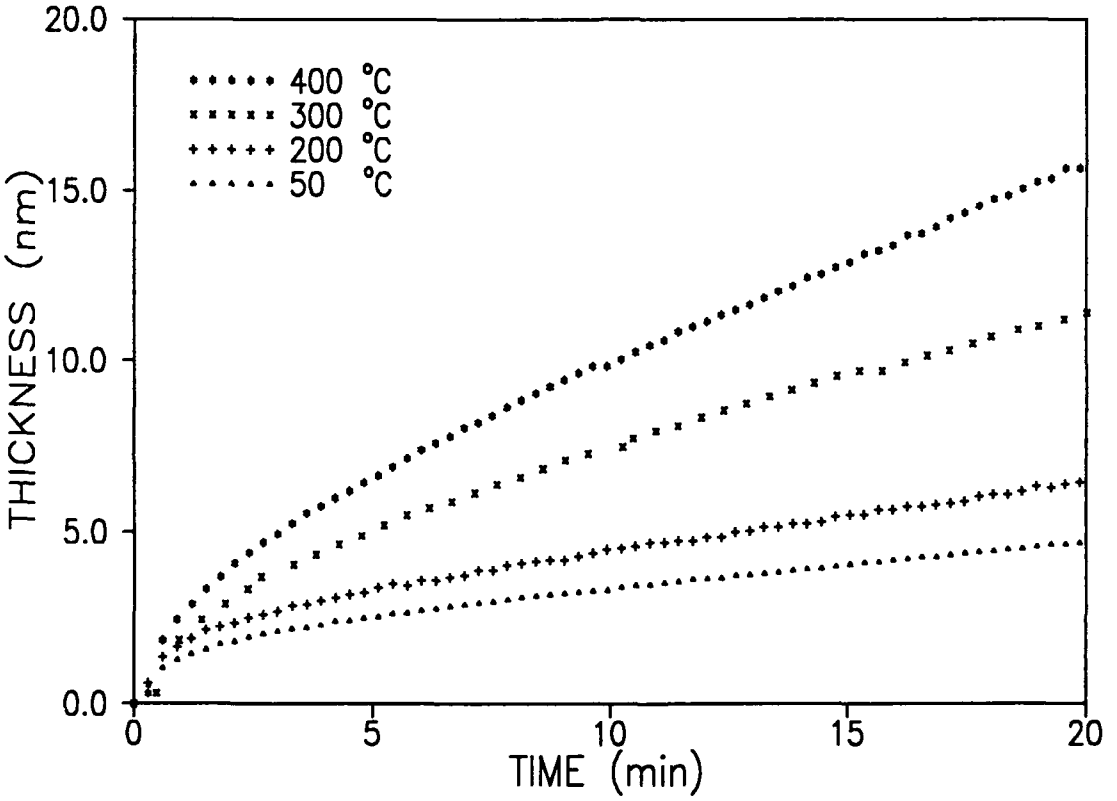
20.0
15.0
10.0
5.0
0.0
THICKNESS (nm)
400 °C
300 °C
200 °C
50 °C
0
5
10
15
20
TIME (min)

Fig. 8

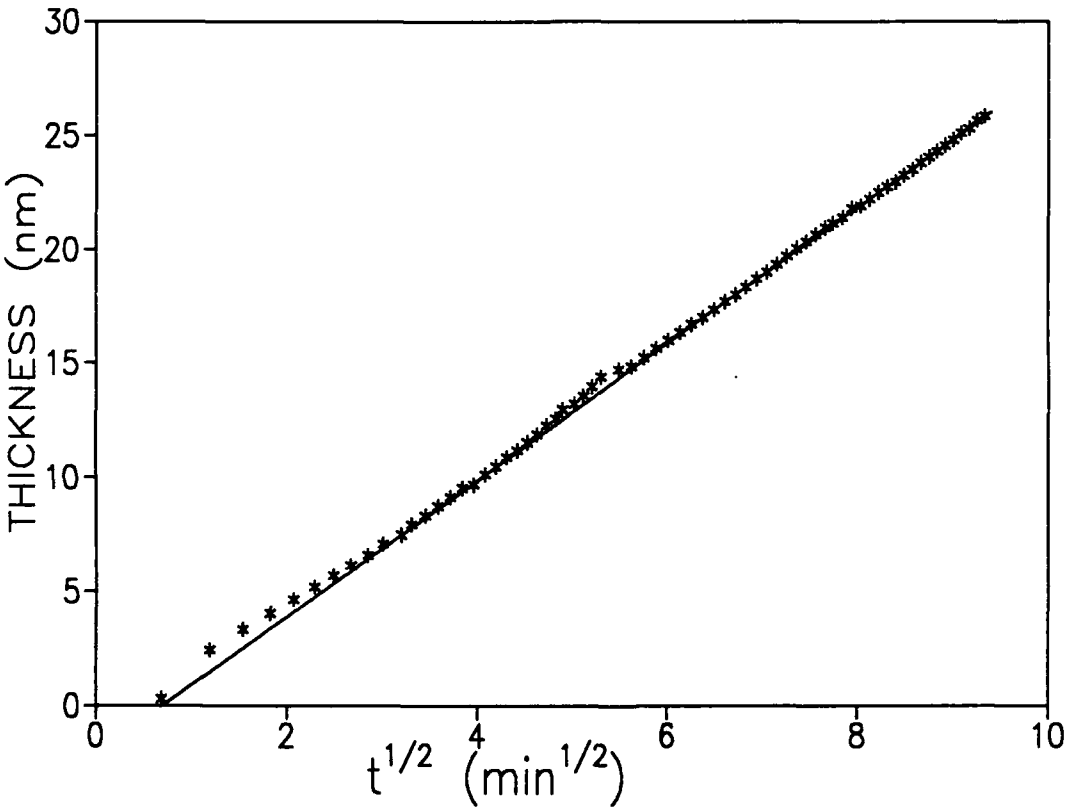

Fig. 9

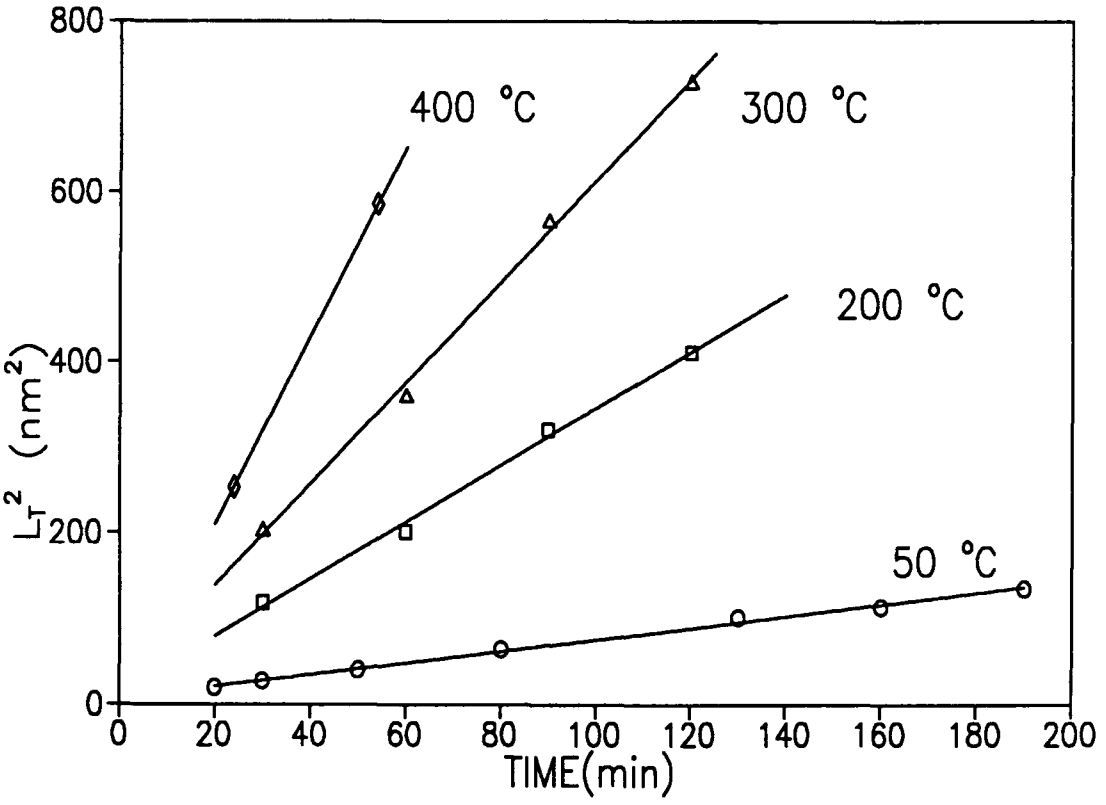
800
600
400
200
0
L_T^2 (nm^2)
400 °C
300 °C
200 °C
50 °C
0
20
40
60
80
100
120
140
160
180
200
TIME(min)

Fig 10

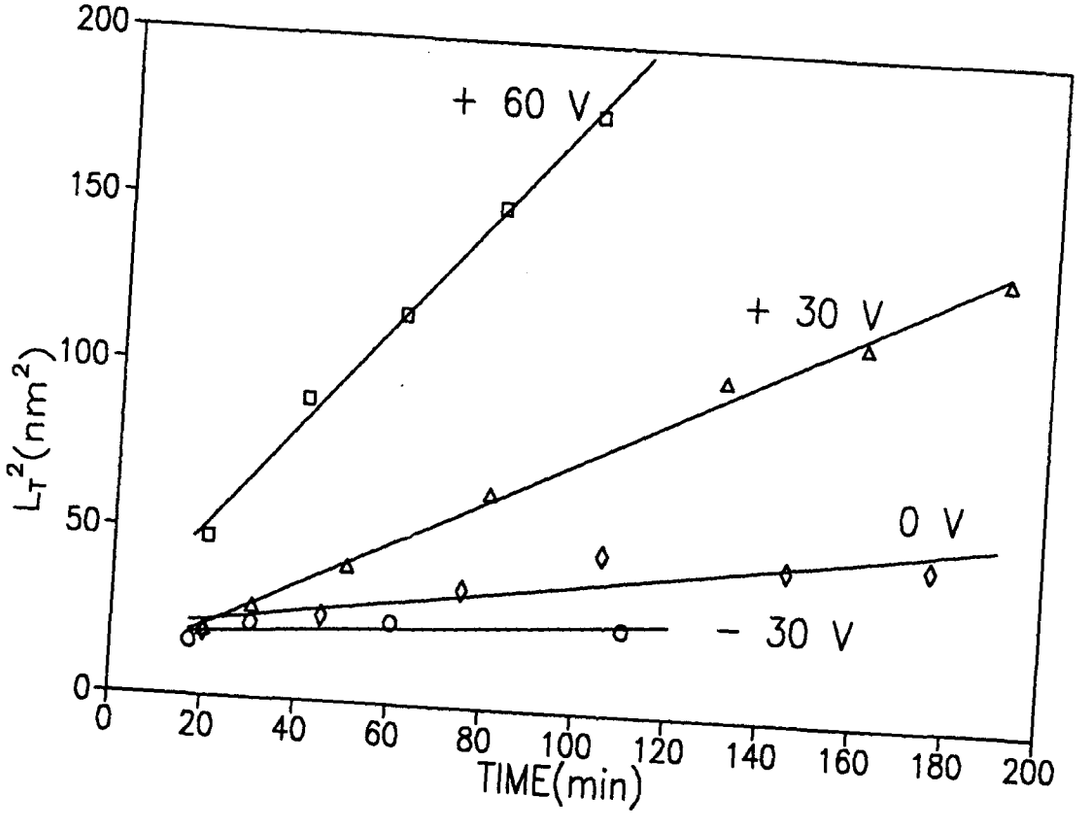
200
150
100
50
0
$L_T^2(nm^2)$
+ 60 V
+ 30 V
0 V
- 30 V
0
20
40
60
80
100
120
140
160
180
200
TIME(min)

Fig 11

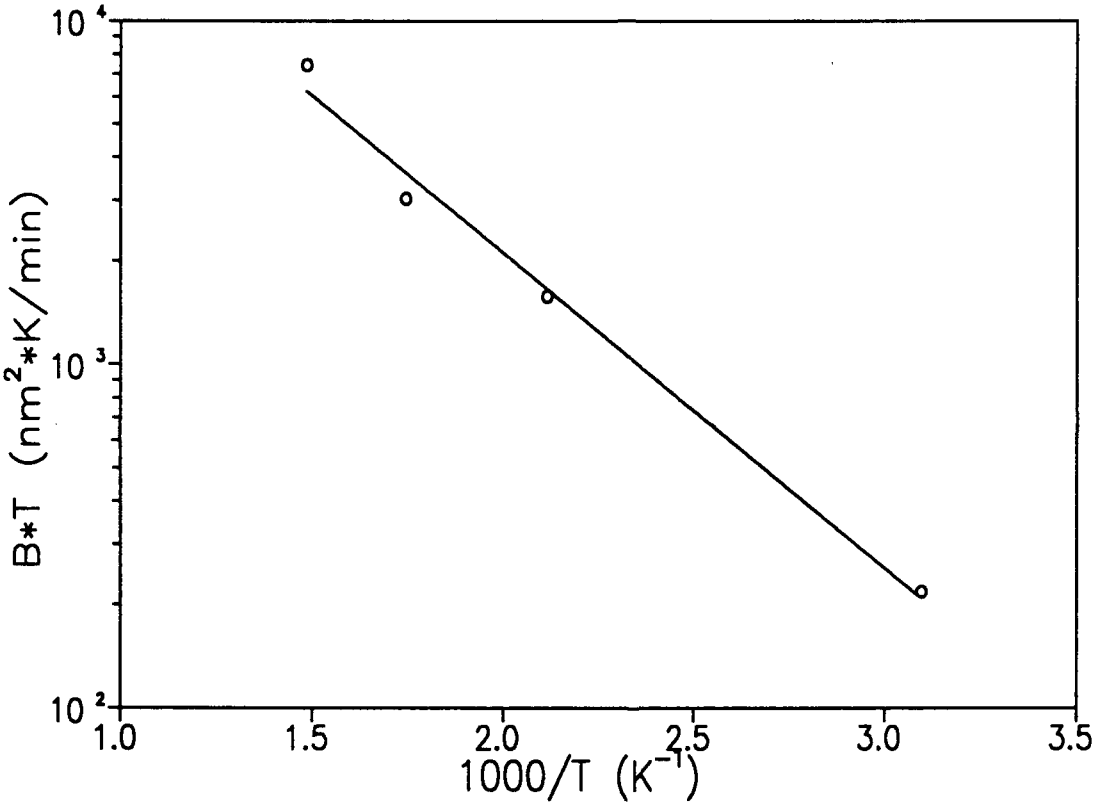

F, 12

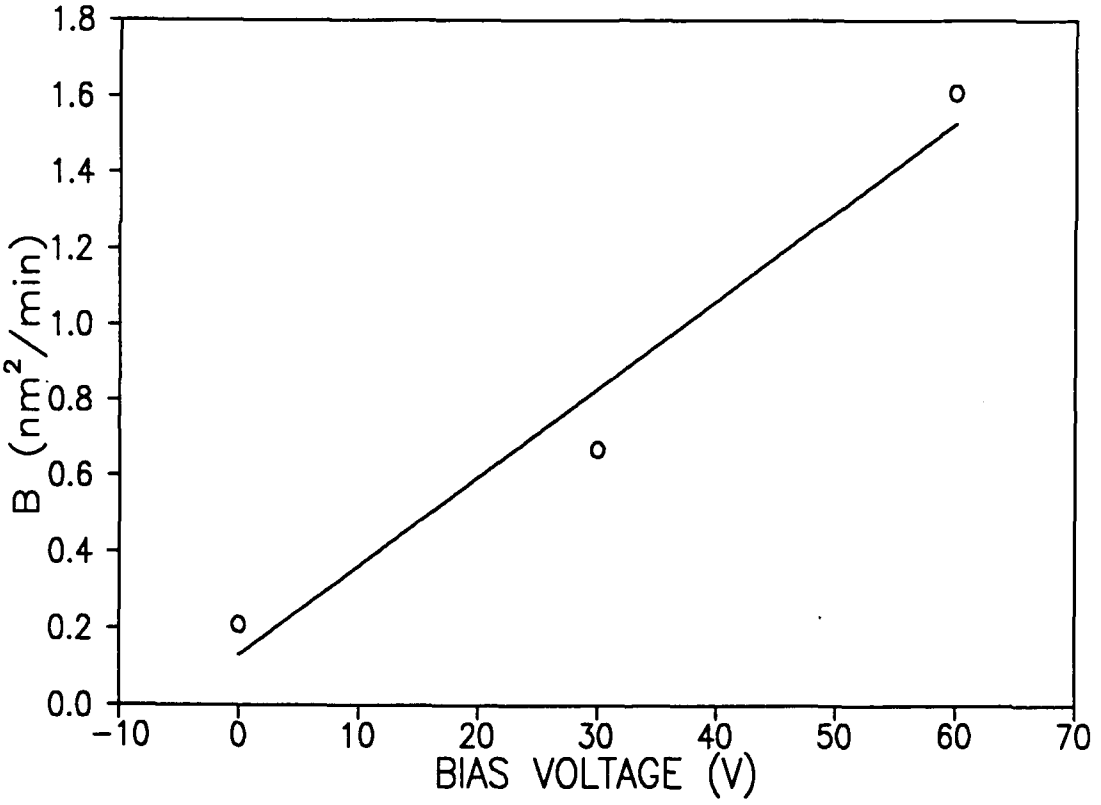
1.8
1.6
1.4
1.2
1.0
0.8
0.6
0.4
0.2
0.0
B (nm²/min)
−10
0
10
20
30
40
50
60
70
BIAS VOLTAGE (V)

Fig. 13